Prev. Nutr. Food Sci. 2021;26(1):58-66
https://doi.org/10.3746/pnf.2021.26.1.58
ISSN 2287-8602

Ergostatrien-3β-ol (EK100) from *Antrodia camphorata* Attenuates Oxidative Stress, Inflammation, and Liver Injury *In Vitro* and *In Vivo*

Ting-Yu Chao[1]*, Cheng-Chu Hsieh[2]*, Shih-Min Hsu[1,3]*, Cho-Hua Wan[4], Guan-Ting Lian[1], Yi-Han Tseng[1], Yueh-Hsiung Kuo[5], and Shu-Chen Hsieh[1]

[1]Institute of Food Science and Technology, [4]Department and Institute of Veterinary Medicine, School of Veterinary Medicine, and [5]Department of Chemistry, National Taiwan University, Taipei 106, Taiwan
[2]Biologics Division, Animal Health Research Institute, Council of Agriculture, Executive Yuan, New Taipei 251, Taiwan
[3]Metal Industries Research and Development Centre, Kaohsiung 811, Taiwan

ABSTRACT: Hepatic ischemia/reperfusion (IR) injury is a complication that occurs during liver surgery, whereby hepatic tissue is injured by oxygen deficiency during ischemia, then further damaged by a cascade of inflammatory and oxidative insults when blood is resupplied during reperfusion. *Antrodia camphorata* is an indigenous fungus in Taiwan and an esteemed Chinese herbal medicine with various bioactivities. This study examined the effect of ergostatrien-3β-ol (EK100), an active compound found in both the fruiting body and mycelia of *A. camphorata*, on IR injury pathologies in rats and cell models of oxidative and inflammatory stress. Male Sprague-Dawley rats were randomly assigned to receive a vehicle or 5 mg/kg EK100 prior to hepatic IR injury induced by 1 h ischemia followed by 24 h reperfusion, or a sham operation. RAW 264.7 murine macrophages and HepG2 hepatocytes were pretreated with EK100, then inflammation was induced with lipopolysaccharides in the former and oxidative stress was induced with hydrogen peroxide in the latter. EK100 decreased IR-induced elevation in serum levels of alanine aminotransferase and aspartate aminotransferase and lowered levels of the inflammatory cytokines tumor necrosis factor-α, interleukin (IL)-6, and IL-1β. In addition, EK100 significantly reduced hepatic mRNA levels of inducible nitric oxide synthase (iNOS) and cyclooxygenase-2, as well as nitrite production and iNOS gene expression in both hepatocyte and macrophage cell lines. We demonstrated that EK100 exhibits potent protection against hepatic IR injury, which may be used to design strategies to ameliorate liver damage during liver surgery.

Keywords: anti-inflammation, EK100, hepatic ischemia/reperfusion injury, hepatoprotection

INTRODUCTION

Chronic liver diseases are a major cause of morbidity and mortality globally (Pillai and Chen, 2016). Although the number of cases of viral hepatitis is effectively reduced by systematic and preventive immunization, the prevalence of metabolic liver diseases such as non-alcoholic steatohepatitis (NASH) and alcohol-related liver disease are on the rise, enhancing the likelihood of progressing into cirrhosis and hepatocellular carcinoma (Sepanlou et al., 2020). The most effective therapy for end-stage liver disease is liver transplant, which has the risk of liver graft failure and post-surgery trauma due to ischemia/reperfusion (IR) injury. Hepatic IR injury occurs as a result of blockage of blood flow to the liver for a variable length of time, followed by progressively violent oxidative and inflammatory insult due to the resupply of blood during reperfusion (Konishi and Lentsch, 2017). The altered redox state of ischemia causes swelling of endothelial cells, hepatocytes, and Kupffer cells, which reduces microcirculatory blood flow and mitochondrial ATP production (Weigand et al., 2012). Reperfusion elicits the release of reactive oxygen species (ROS) and chemokines. Then, leukocytes infiltration is accompanied by increased production of inflammatory cytokines, including tumor necrosis factor (TNF) and interleukins (IL), as well as nitric oxide (NO) and ROS. This causes apoptosis and necrotic death of liver parenchyma and may lead to remote organ

Received 21 August 2020; Revised 15 October 2020; Accepted 25 November 2020; Published online 31 March 2021

Correspondence to Shu-Chen Hsieh, Tel: +886-2-3366-9871, E-mail: scjhsieh@ntu.edu.tw
*These authors contributed equally to this work.
Author information: Ting-Yu Chao (Graduate Student), Shih-Min Hsu (Graduate Student), Cho-Hua Wan (Professor), Guan-Ting Lian (Graduate Student), Yi-Han Tseng (Graduate Student), Yueh-Hsiung Kuo (Professor), and Shu-Chen Hsieh (Professor)

failure, greatly threatening patient prognosis (de Groot and Rauen, 2007). One of the strategies to lessen IR injury is preconditioning with pharmacological agents to directly or indirectly neutralize the effects of injurious molecular disturbances pertaining to hepatic IR injury (Nickkholgh et al., 2012).

Antrodia camphorata is an endemic fungus that grows in cavities of rotten trunks of *Cinnamomum kanehirai*, native to Taiwan. It is considered one of the most precious Chinese herbal medicines due to its rarity, and has been highly praised as a remedy for food poisoning, diarrhea, stomach ache, hypertension, itchy skin, and liver illness (Hsieh et al., 2015; Yang et al., 2017). In addition, many studies have shown that *A. camphorata* possesses a wide range of biological activities, including anti-cancer, anti-oxidation, lipid homeostasis, hepatoprotection, vasorelaxation, and immunomodulation (Chang et al., 2011; Geethangili and Tzeng, 2011; Wu et al., 2011; Liu et al., 2012; Tsai et al., 2015; Chang et al., 2017). In particular, liver protection is regarded as its most exceptional bioactive property. Ergostatrien-3β-ol (EK100), found in both the fruiting body and mycelia of *A. camphorata*, is one of its active compounds; nevertheless, the potential of this compound to protect against hepatic IR injury has not been investigated.

In this study, we recreated liver IR injury in rats and induced oxidative and inflammatory stress in hepatic and macrophage cell lines to investigate the hepatoprotection offered by EK100 in both *in vivo* and *in vitro* models.

MATERIALS AND METHODS

Preparation of EK100

Isolation and determination of EK100 from *A. camphorata* was performed as described by Shao et al. (2008). Briefly, the freeze-dried powder of *A. camphorata* liquid fermentation broth was extracted three times with ethanol at room temperature. The extract was then evaporated *in vacuo*, suspended in H_2O, and partitioned three times each with 1 L of ethyl acetate (EtOAc). The EtOAc fractions were separated on silica gel using hexane and EtOAc in different proportions to create eluents of increasing polarity. The eluates were further purified with high-performance liquid chromatography. EK100 was eluted with 10% EtOAc in hexane.

Liver IR injury animal model

Male Sprague-Dawley rats (weighing 250～300 g) were housed in polycarbonate cages, and received standard rodent diet (LabDiet 5001, Purina Mills Inc., St. Joseph, MO, USA) and clean water ad libitum. Rats were kept at 23±2°C, 60±10% relative humidity, and 12 h light/dark cycle. Prior to the experiment, rats were acclimatized for two weeks and randomly divided into three groups (n=6): (1) control group: sham operation, (2) vehicle-treated IR injury 24 h group (IR24), (3) EK100-treated IR injury 24 h group (IR24+EK100). EK100 was dissolved in 1% carboxymethylcellulose (Sigma-Aldrich Co., St. Louis, MO, USA).

At 1 h before ischemia, rats in the sham and IR24 groups were administered a vehicle (1% carboxymethylcellulose), whereas the EK100 group was given 5 mg/kg EK100 by intraperitoneal injection. The dose of EK100 was determined from previous literature (Huang et al., 2010) and a preliminary study conducted in our lab. After anesthesia with isoflurane (1～2%, inhalation route) and midline laparotomy, the liver was exposed through an upper midline incision and two pieces of fine silk thread were looped along the right and left branches of the portal vein, hepatic artery, and bile duct. Hepatic ischemia was induced by clamping the pedicles of the left and middle lobes for 1 h. After the silk threads were removed, reperfusion was initiated. Blood pressure was monitored by tail vein sphygmomanometer throughout the operation. At 24 h after reperfusion, rats were sacrificed and the liver tissues and blood samples were collected. The study protocol was approved by the Institutional Animal Care and Use Committee of National Taiwan University (IACUC No. NTU-98-EL-109) in compliance with the Guide for the Care and Use of Laboratory Animals (National Research Council, 2011).

Histological analysis

Fresh liver tissues were fixed in formalin, processed through standard histological procedures, and then embedded in paraffin. Tissue sections (4～5 μm) were cut and stained with hematoxylin and eosin (H&E). H&E stained slides were imaged at 40×, 100×, 200×, and 400× magnification with a microscope (Nikon Eclipse Ni, Nikon, Tokyo, Japan). Pathophysiological damage to the liver was assessed according to Rao et al. (2013) by two independent histologists.

Measurement of serum alanine aminotransferase (ALT) and aspartate aminotransferase (AST) activities

Blood samples were allowed to clot at room temperature for 30 min, then were centrifuged at 3,000 *g* for 5 min. Supernatants were collected and designated as serum. Serum ALT and AST levels were measured by a SPOTCHEM SP-4410 clinical chemistry analyzer (ARKRAY, Inc., Kyoto, Japan).

Biochemical analysis

Hepatic levels of superoxide dismutase (SOD) and serum levels of IL-1β, IL-6, and TNF-α were determined using commercial assay kits (SOD: Cat. No. 19160; IL-1β, IL-6, and TNF-α: Cat. No. RAB0277, RAB0311, and RAB0479,

respectively; Sigma-Aldrich Co.) according to the manufacturers' instructions.

Total RNA extraction and reverse transcription-quantitative polymerase chain reaction (RT-qPCR)

Total RNA was extracted from liver tissues or isolated from cells by TriPure Isolation Reagent (Roche Applied Science, Penzberg, Germany) according to the manufacturer's instructions. RNA (5 μg) was reversed transcribed to cDNA using random hexamer primers and SMART MMLV Reverse Transcriptase (Takara Bio USA, Inc., Mountain View, CA, USA) according to the manufacturer's protocol. Quantitative PCR was performed on StepOnePlus™ Real-Time PCR Systems (Applied Biosystems, Waltham, MA, USA) using KAPA SYBR® FAST qPCR kits (Roche Diagnostics, Indianapolis, IN, USA). RT-qPCR was performed using the primers listed in Table 1.

Western blot analysis

Liver tissue was minced with a handheld homogenizer and then incubated in radioimmunoprecipitation assay buffer [50 mM Tris (pH 7.5), 150 mM NaCl, 1% Triton X®-100, 1% sodium deoxycholate, and 0.1% sodium dodecyl sulfate (SDS)] containing Halt protease and phosphatase inhibitor cocktail for 30 min, with vortexing every 10 min. The protein content was quantified using Bradford protein assays, and 30 μg of protein extracts were separated using SDS-polyacrylamide gel electrophoresis on 10% or 12% gel. The separated proteins were transferred to polyvinylidene fluoride membranes, and membranes were blocked in 5% skim milk in Tris-buffered saline (TBS) with 5% Tween-20 (TBS-T). The membranes were incubated overnight at 4°C with primary antibodies (Santa Cruz Biotechnology Inc., Dallas, TX, USA), heme-oxygenease (HO-1) at 1:500 or β-actin at 1:1,000 diluted in TBS-T containing 5% bovine serum albumin. After incubation with horseradish peroxidase-conjugated anti-mouse or anti-rabbit immunoglobulin (GeneTex Inc., Irvine, CA, USA) for 1 h at room temperature, protein bands were visualized using a bioimaging system (Analytik Jena US LLC., Upland, CA, USA) with chemiluminescent detection kit (T-Pro Biotechnology, New Taipei, Taiwan). Bands were quantified using ImageJ, an open source software developed by the National Institutes of Health.

Time-course *HO-1* mRNA expression under H_2O_2-induced oxidative stress

HepG2 cells was maintained in Dulbecco's modified Eagle's medium (DMEM; Thermo Fisher Scientific, Waltham, MA, USA) supplemented with 10% fetal bovine serum, 25 mM sodium bicarbonate, 12.5 mM hydroxyethyl piperazine ethane sulfonic acid, 4 mM L-glutamine, 1 mM sodium pyruvate, and 25 mM glucose. Cells were treated with 10 μM EK100 for 17 h, followed by 1 mM H_2O_2 for induction of oxidative stress for 6 and 12 h. Total RNA was isolated and *HO-1* gene expression was detected as described previously. Representative data from at least three independent experiments are shown.

Anti-inflammatory effect of EK100 under LPS-induced inflammation

RAW 264.7 was maintained in DMEM supplemented with 10% fetal bovine serum, 25 mM sodium bicarbonate and 25 mM glucose. Cells were pretreated with EK100 at concentrations of 1, 2, and 5 μM for 1 h, and then treated with lipopolysaccharide (LPS) (1 μg/mL) for 12 h before the cell medium or cell lysate was collected and nitrite or inducible NO synthase (iNOS) mRNA levels were measured. Nitrite levels were measured using the Griess method. Briefly, 100 μL cell supernatant was loaded (in duplicate) into a 96-well plate, followed by addition of 50 μL Griess I reagent (1% sulfanilamide in 5% phosphoric acid) and 50 μL Griess II reagent (0.1% naphthylethylenediamine dihydrochloride in water). After mixing thoroughly, the plate was incubated for 10 min at room temperature and absorbance was measured at 550 nm. For iNOS mRNA expression, total RNA was isolated and gene expression was detected as described previously using forward and reverse primers listed in Table 1. For nuclear factor (NF)-κB transcriptional activity, stable RAW 264.7 clones transfected with a plasmid containing NF-κB response element and a luciferase reporter gene were pretreated with EK100 at 1, 2, and 5 μM for 1 h

Table 1. Sequences of primers used for RT-qPCR

Genes	Forward (5′→3′)	Reverse (5′→3′)
Rat 18S	TAT TCC CAT GAC CCG CC	GTG AGG TTT CCC GTG TT
Rat iNOS	CCA GGA GAT GTT GAA CTA CG	CGC ATT AGC ACA GAA GCA AA
Rat COX-2	GTC TTT GGT CTG GTG CC	TCA CTA TCT TGA TCG TCT CTC CTA
Rat HO-1	GCT CTA TCG TGC TCG CAT GA	AAT TCC CAC TGC CAC GGT C
Rat NQO1	ACT CGG AGA ACT TTC AGT ACC	TTG GAG CAA AGT AGA CTG GT
Human HO-1	AAC TTT CAG AAG GGC CAG GT	CTG GGC TCT CCT TGT TGC
Mouse iNOS	CCT GGT ACG GGC ATT GCT	GCT CAT GCG GCC TCC TTT

iNOS, inducible nitric oxide synthase; COX-2, cyclooxygenase-2; HO-1, heme oxygenase-1; NQO1, nicotinamide adenine dinucleotide phosphate hydrate quinone oxidoreductase 1.

and then induced by LPS (1 μg/mL) for 6 h. Cell lysates were collected, added to the substrate, and luciferase activity was immediately measured using a luminometer (Luminoskan, Thermo Scientific, Waltham, MA, USA).

Statistical analysis

Results are expressed as mean±standard deviation (SD). Statistical significance was defined as $P<0.05$ by one-way analysis of variance (ANOVA) and Duncan's multiple range test. Data were analyzed using SigmaPlot (Sigma-Aldrich Co.) and graphs were drawn using GraphPad Prism 7 (GraphPad Software, San Diego, CA, USA).

RESULTS

Effects of EK100 on ALT and AST levels, and liver histology

We recreated hepatic IR injury in rats by employing 1 h of median/left lobar ischemia followed by 24 h of reperfusion. Compared to the control group, rats subjected to IR injury showed a dramatic increase in serum ALT and AST levels (2,780.0±723.3 IU/L and 4,456.7±1,533.3 IU/L, respectively versus 38.7±8.6 IU/L and 72.8±19.6 IU/L, respectively in controls), indicating significant damage to the liver. Treatment with 5 mg/kg EK100 markedly attenuated serum ALT and AST levels to 79.3±19.6 IU/L and 205±13.3 IU/L, respectively (Fig. 1A). Liver sections of IR rats exhibited severe coagulative necrosis, whereas EK100 restored normal liver architecture to levels in the control group (Fig. 1B).

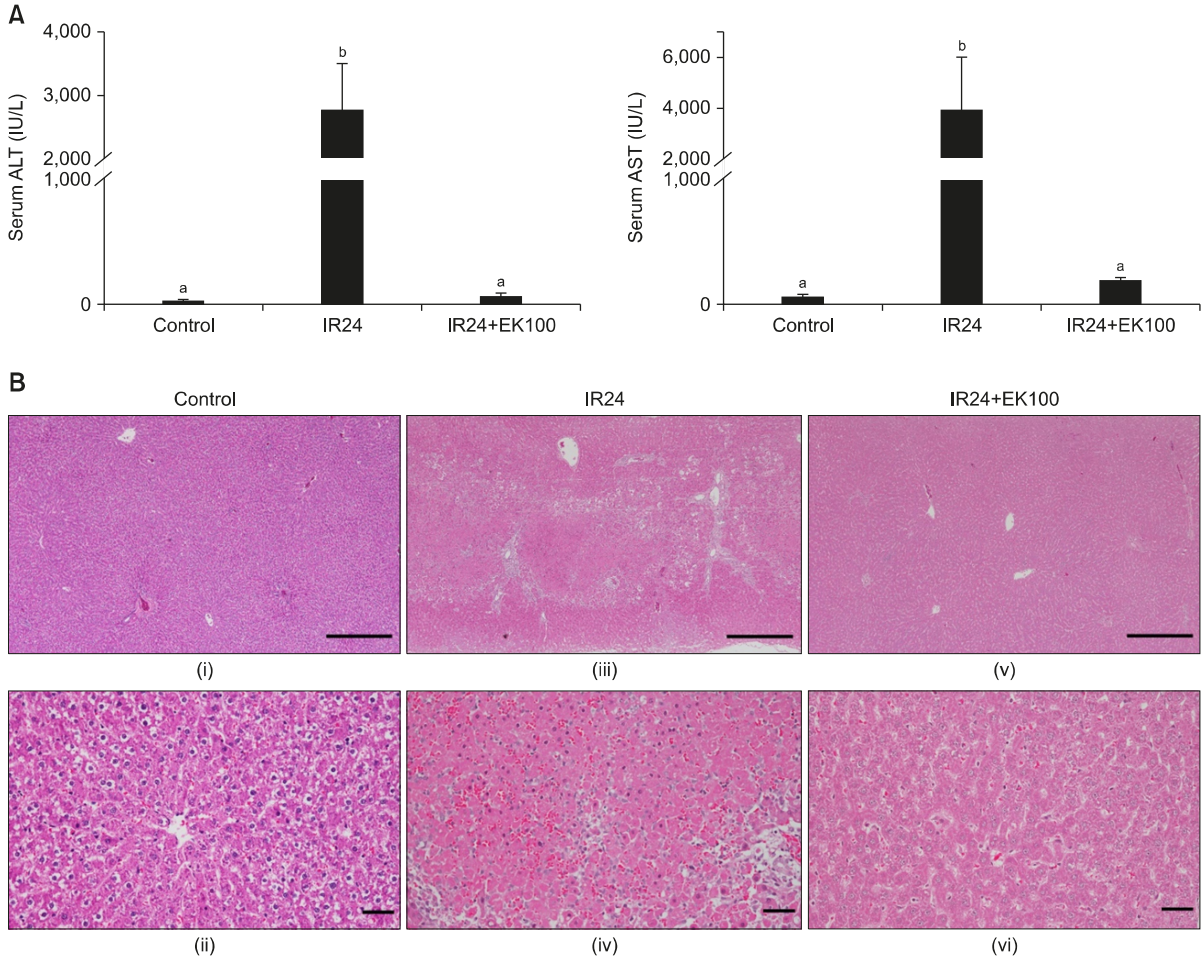

Fig. 1. Effects of ergostatrien-3β-ol (EK100) on (A) serum activities of alanine aminotransferase (ALT), aspartate aminotransferase (AST), and (B) histological sections from liver of ischemia/reperfusion (IR)-induced hepatic injury in rats. Rats (n=6) were pretreated with EK100 (5 mg/kg, i.p.) or vehicle, followed by 1 h of liver ischemia and 24 h of reperfusion before sacrifice. (A) Bars marked with different letters (a,b) are significantly different, as determined by one-way ANOVA and Duncan's multiple comparisons test ($P<0.05$). Values are mean±SD (n=6). (B) IR24 (iii and iv) shows moderate degenerative lesions along with large areas of coagulative necrosis compared to the control (i and ii), which has distinct nuclei and cytoplasm. IR24+EK100 (v and vi) shows significantly improved morphology with mild (2~5%) degenerative lesions and slight hemorrhage. Photographs of H&E stain taken at 40× magnification (i, iii, and v), scale bar=500 μm and 200× (ii, iv, and vi), scale bar=50 μm. Representative images from histopathological analysis are shown.

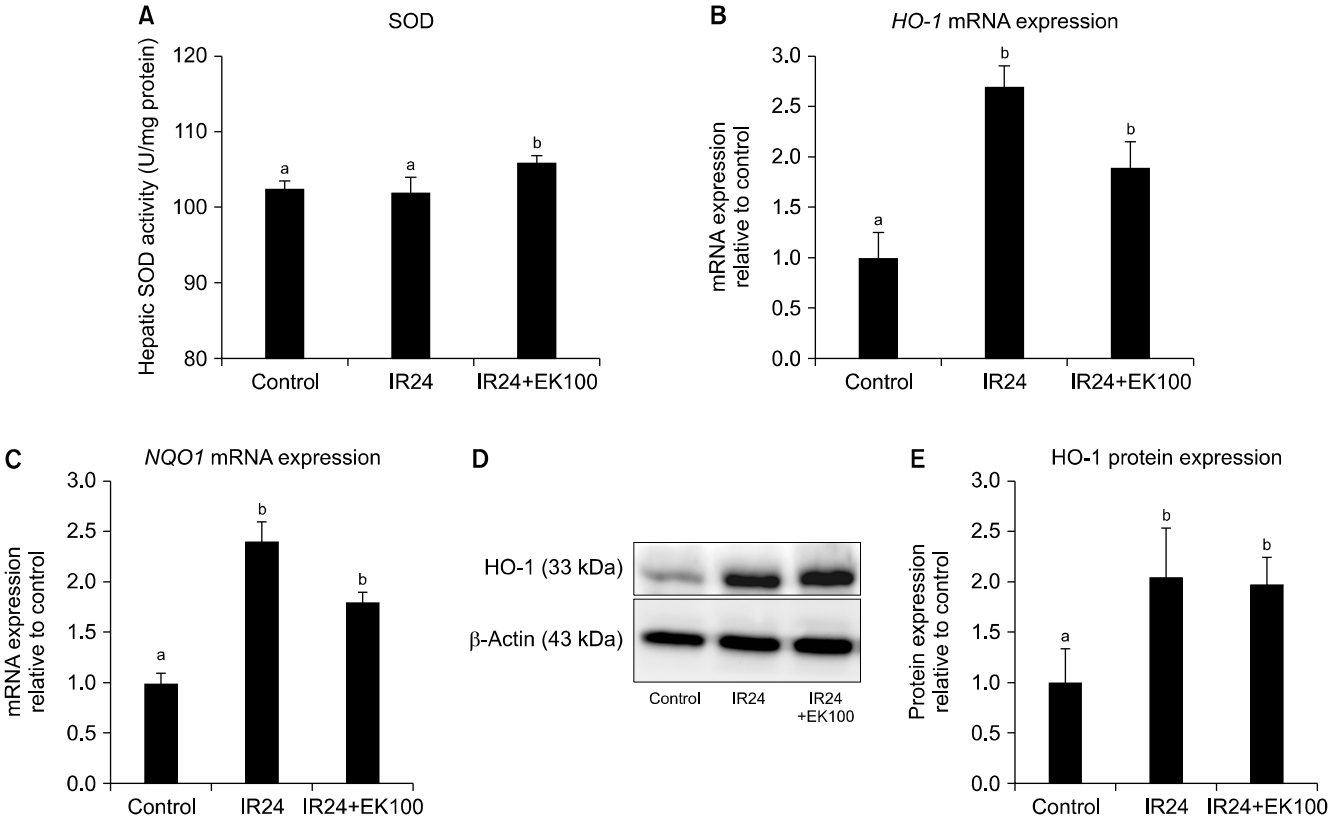

Fig. 2. Effects of ergostatrien-3β-ol (EK100) on (A) liver superoxide dismutase (SOD) activity, (B) heme-oxygenase (HO)-1 mRNA levels, (C) nicotinamide adenine dinucleotide phosphate hydrate quinone oxidoreductase 1 (NQO1) mRNA levels, and (D and E) HO-1 protein expression in hepatic ischemia/reperfusion (IR) injury in rats. (A) One milligram of liver tissue was homogenized in assay buffer and SOD activity was measured following the manufacturer's protocol. (B and C) Equal amounts of hepatic total RNA extracts were reverse-transcribed and cDNA was quantified by qPCR with HO-1 and NQO1 primers. 18S was used as an internal control. (D) Equal amounts of hepatic protein extracts were separated by SDS-PAGE and analyzed by Western blot with HO-1 antibody. β-Actin was used as an internal control. (E) Quantification of bands from (D). Bars marked with different letters (a,b) are significantly different as determined by one-way ANOVA and Duncan's multiple range test ($P<0.05$). Values are mean±SD (n=6). A representative image of the protein bands is shown.

Anti-oxidative effects of EK100

SOD activity significantly increased in EK100-treated rats compared to IR rats (Fig. 2). Moreover, EK100 significantly elevated hepatic *HO-1* and nicotinamide adenine dinucleotide phosphate hydrate quinone oxidoreductase 1 (*NQO1*) gene expression and HO-1 protein levels compared with the control group. However, there was no significant difference between the IR and EK100 groups.

Anti-inflammatory effects of EK100

In the IR group, inflammatory molecules, including hepatic *iNOS* and *cyclooxygenase* (*COX*)-*2* gene expression, and serum cytokine levels (IL-1β, IL-6, and TNF-α) were significantly increased compared with the control, indicating a highly activated immune response against liver damage caused by ischemia and reperfusion (Fig. 3). The inflammatory response was effectively decreased by EK100 treatment.

Effects of EK100 on cellular oxidative stress and inflammation

We later examined whether EK100 can rescue H_2O_2-induced oxidative stress in a hepatocyte cell line. In our preliminary study, treatment of HepG2 cells with EK100 (10 μM) at different time points (0, 2, 4, 8, 12, 17, and 24 h) caused *HO-1* mRNA expression to gradually increase, reaching a maximum at 17 h (data not shown). Thus, in this study, HepG2 cells were treated with EK100 at 10 μM for 17 h, and then with 1 mM H_2O_2 for 6 or 12 h to induce oxidative stress. Under oxidative stress, *HO-1* mRNA levels significantly increased approximately 3.3-fold compared with the control group (Fig. 4A). EK100 treatment further increased *HO-1* mRNA expression by approximately 7.5-fold compared with the control. However, the expression decreased to basal levels with longer induction with H_2O_2, and was slightly enhanced by EK100 after 12 h. Inhibition of inflammatory molecules and signaling in LPS-stimulated RAW 264.7 murine macrophage cell line is considered a quick, non-laborious model to screen various anti-inflammatory drugs. Using this model, NO levels increased significantly to 16.2 μM with LPS, whereas EK100 at different concentrations attenuated NO production in a dose-dependent manner (Fig. 4B). Using luciferase reporter assays, we showed

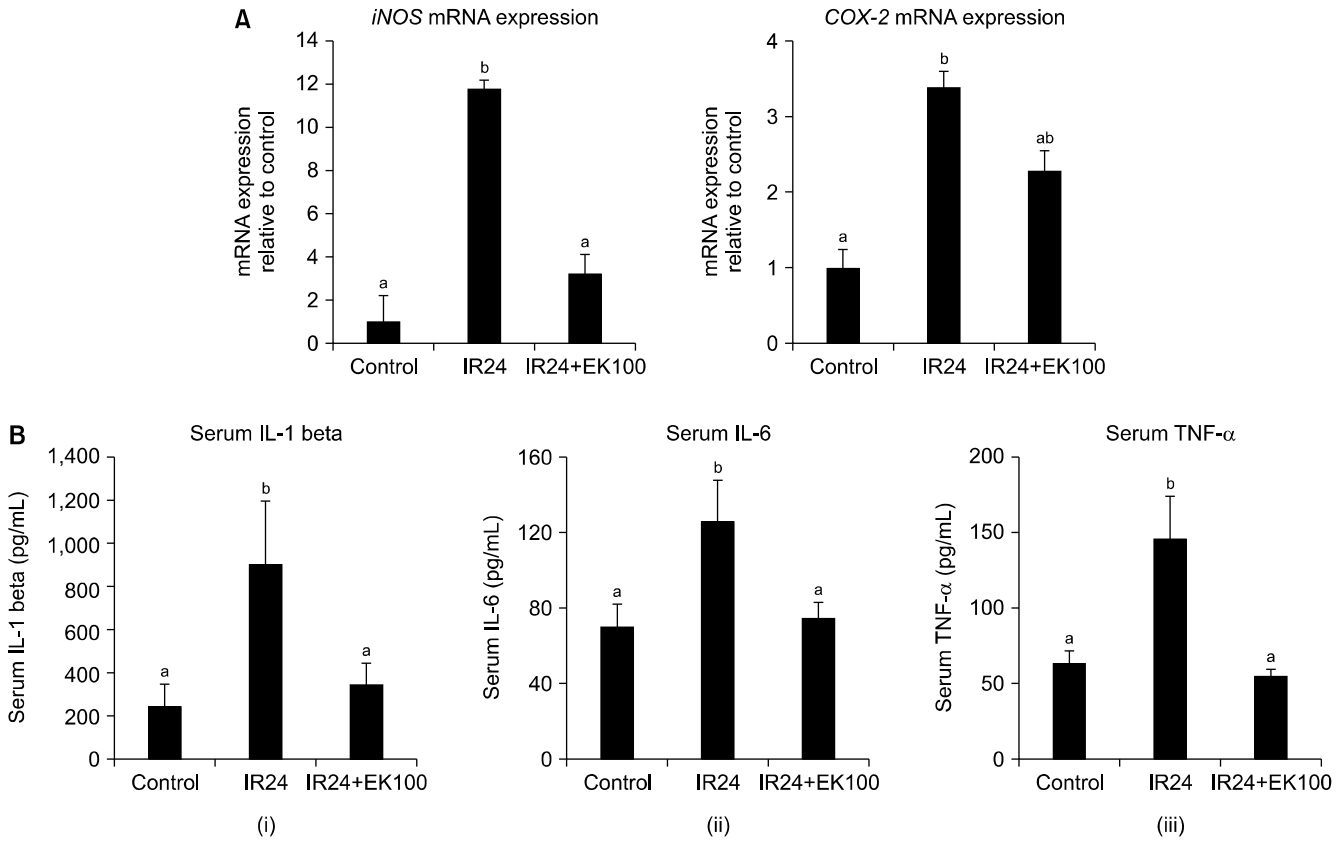

Fig. 3. Inflammatory markers in (A) liver and (B) serum of rats with hepatic ischemia/reperfusion (IR) injury. (A) Equal amounts of hepatic total RNA extracts were reverse-transcribed and cDNA was quantified by qPCR using inducible nitric oxide synthase (iNOS) and cyclooxygenase (COX)-2 primers. 18S was used as an internal control. (B) Serum levels of (i) interleukin (IL)-1β, (ii) IL-6, and (iii) tumor necrosis factor (TNF)-α were determined using ELISA kits. Bars marked with different letters (a,b) are significantly different, as determined by one-way ANOVA followed by Duncan's multiple range test (P<0.05). Values are mean±SD (n=6).

that EK100 significantly decreased LPS-induced increases in iNOS mRNA expression (Fig. 4C), but not NF-κB transcriptional activity (Fig. 4D).

DISCUSSION

Increasing evidence indicates that ROS plays a central role in IR injury by directly attacking hepatocytes or indirectly causing production of inflammatory mediators (Nitescu et al., 2006). In hepatic ischemia and reperfusion injury, ROS activates Kupffer cells and neutrophils, which produces more ROS (Jaeschke and Smith, 1997; Jaeschke, 2003) and activates the innate immune system to release inflammatory cytokines (Land, 2005). TNF-α is a crucial factor that drives the inflammatory cascade by inducing production of cytokines, such as IL-1β and IL-6, with the former causing neutrophil activation and NO upregulation through iNOS and NF-κB-mediated pathways that aggravate liver damage (Cannistrà et al., 2016).

Here, we employed the rat model described by Yamauchi et al. (1982). The duration of ischemia is critical, since short-term (≤20 min) or long-term (≥90 min) ischemia results in little or irreversible functional and structural changes, respectively. Sinusoidal perfusion failure was aggravated when the period of ischemia was prolonged to 60 min (Koo et al., 1992). Therefore, we applied 60 min of median/left lobar ischemia followed by 24 h of reperfusion, which resulted in significant functional alterations (Fig. 1A), providing a reproducible system for studying the protective effect of EK100 on liver against IR injury.

A. camphorata is recognized as a herb with potent bioactivities. EK100, a triterpenoid compound abundant in both the fruiting bodies and mycelia of *A. camphorata*, also shows promising medicinal uses. Kuo et al. (2015) reported the glucose- and lipid-lowering effect of EK100 through its ability to downregulate hepatic fatty acid synthesis and gluconeogenesis in high fat diet-fed mice. Another study revealed that EK100 enhances the activities of the anti-oxidant enzymes catalase, SOD and glutathione peroxidase. In addition, EK100 can decrease TNF-α levels, NO production, and iNOS and COX-2 protein expression in carrageenan-induced paw edema in mice (Huang et al., 2010). Furthermore, topical application of EK100 can inhibit UVB-induced damage by reducing ex-

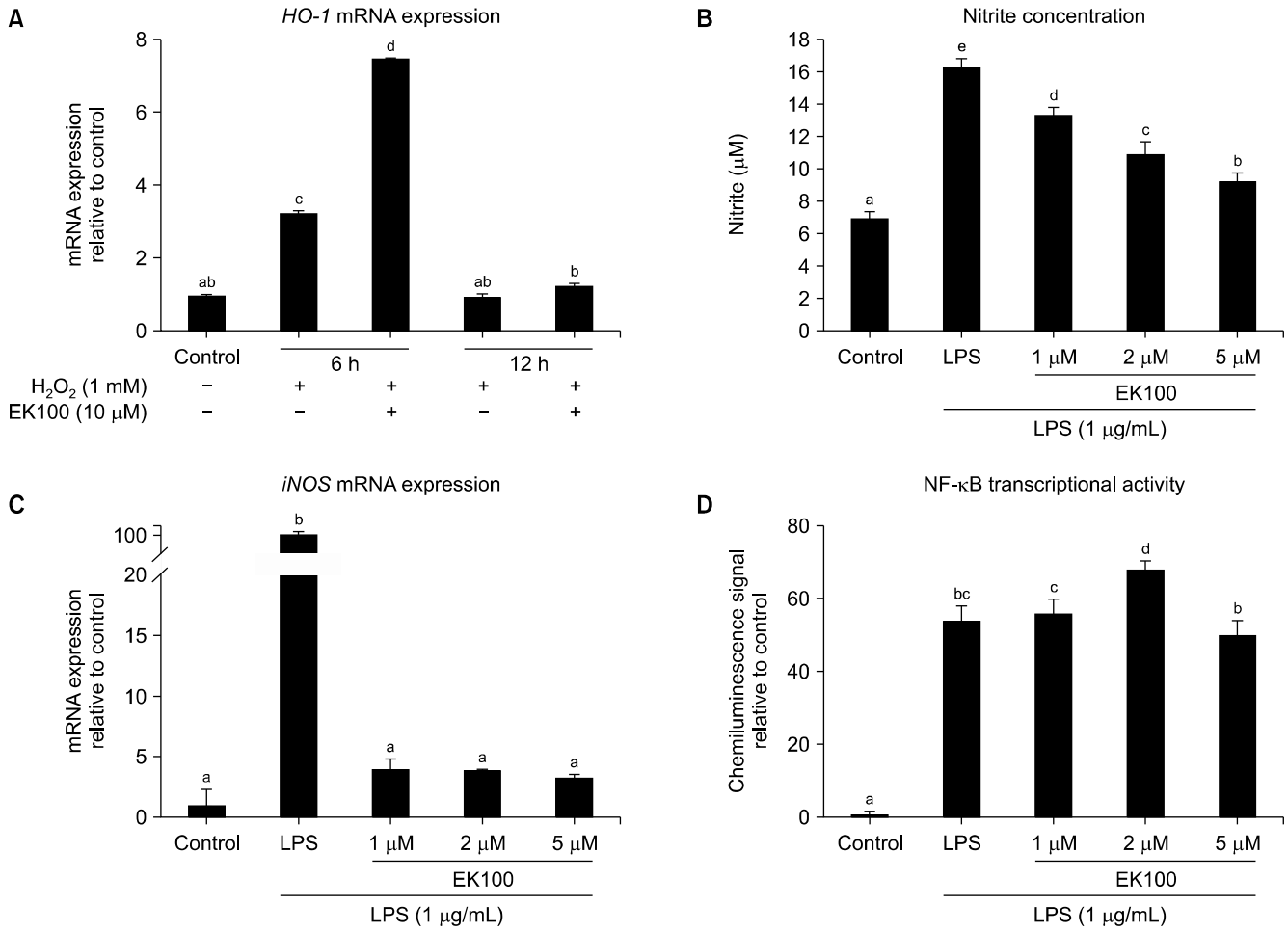

Fig. 4. Effects of ergostatrien-3β-ol (EK100) on (A) mRNA expression of heme-oxygenase (HO)-1 in HepG2 cells, and (B) nitric oxide (NO) production, (C) inducible NO synthase (iNOS) mRNA, and (D) nuclear factor (NF)-κB transcriptional activity in RAW 264.7 cells. (A) HepG2 cells were treated with EK100 at 10 μM for 17 h, followed by 1 mM H_2O_2 for 6 and 12 h. (B~D) RAW 264.7 cells were pretreated with EK100 at the indicated concentrations for 1 h, followed by LPS for 12 h (B~C) or 6 h (D) after which the cell medium was collected and measured for (B) nitrite levels, or (C) total RNA was collected to measure mRNA expression of iNOS, or (D) cell lysates were collected to assess NF-κB transcriptional activity by luciferase reporter assays. Bars marked with different letters (a-e) are significantly different, as determined by one-way ANOVA and Duncan's multiple range test (P<0.05). Values are mean±SD from at least three independent experiments.

pression of matrix metalloproteinase (MMP)-1, IL-6, iNOS, and NF-κB in mouse skin (Kuo et al., 2015). The abovementioned literature has provided the basis of the anti-inflammatory and anti-oxidative potential of EK100. We therefore examined whether such a benefit is also found in a model of hepatic IR injury.

This study showed that EK100 can restore levels of liver injury indicators ALT and AST to basal levels, implying the lessening of liver damage. In histological analysis, IR injury caused large areas of coagulative necrosis (Fig. 1B) in the liver, while the cellular structure from EK100-treated rats were improved significantly. We further investigated involvement of oxidative stress and inflammatory mediators, and the impact of EK100. Hepatic SOD activity was significantly increased by EK100 treatment (Fig. 2A). There was a non-significant increase in HO-1 protein expression in the EK100 group compared with the IR group. HO-1 has been implicated in protection against oxidative stress and hepatic IR injury (Bauer and Bauer, 2002; Srisook et al., 2005; Liu and Qian, 2015; Li et al., 2019). Indeed, a previous study reported that HO-1 activity peaked at 4~6 h after reperfusion, and then gradually decreased (Yun et al., 2010). We speculated that at the time of analysis HO-1 activity had already decreased from a higher level in the EK100 group.

In HepG2 cells, H_2O_2-induced oxidative stress caused *HO-1* mRNA expression to increase at 6 h and then decrease at 12 h (Fig. 4A). We propose that EK100 treatment can enhance HO-1 expression at an early stage of reperfusion, which could confer protection against IR-induced damage, then HO-1 expression gradually decreases when oxidative stress has been alleviated (at the time of sacrifice).

Inflammatory mediators are an important cause of significant liver injury following initial damage to the liver parenchyma and vasculature caused by ROS secreted by

activated Kupffer cells (Walsh et al., 2009). In our study, inflammatory cytokines (TNF-α, IL-1β, and IL-6) and *iNOS* and *COX-2* mRNA expression in the liver were increased in the IR group, and were significantly reduced by EK100 treatment (Fig. 3). A similar observation was observed in murine macrophage RAW 264.7 cells, confirming the anti-inflammatory effects of EK100 in immune cells, which amounted to reduced IR injury. In LPS-activated RAW 264.7 cells, NO production, NF-κB transcriptional activity and *iNOS* mRNA expression were increased. Pretreatment of EK100 1 h before induction attenuated LPS-induced elevation in nitrite levels and *iNOS* mRNA expression, but there was no significant difference in NF-κB transcriptional activity compared with no EK100 treatment (Fig. 4B∼D). We speculated that EK100 attenuates nitrite levels and *iNOS* mRNA expression, likely through HO-1 since HO-1 was upregulated by EK100 treatment (Fig. 4A) but not via NF-κB (Alcaraz et al., 2004).

This study employed a rat model of hepatic ischemia and reperfusion injury, and cell models of chemically induced oxidative stress and inflammation to provide evidence for the hepatoprotective effects of EK100, which can be attributed to its anti-inflammatory action and anti-oxidative capacity. Inflammation has relevance in many diseases, such as diabetes (Donath and Shoelson, 2011), lipidemia, atherosclerosis (Taleb, 2016), Alzheimer's disease (Bossy-Wetzel et al., 2004; Rubio-Perez and Morillas-Ruiz, 2012), and metabolic disorders (Esser et al., 2014; Rani et al., 2016). It may be beneficial to conduct further studies on the potential of EK100 in these diseases. Our results show that pretreatment with EK100 may provide new hepatoprotective strategies for preventing ischemic hepatitis and damage associated with liver surgery.

ACKNOWLEDGEMENTS

This project is supported by the Ministry of Science and Technology, Taiwan, ROC, fund ID 107-2320-B-002-003-MY3.

AUTHOR DISCLOSURE STATEMENT

The authors declare no conflict of interest.

REFERENCES

Alcaraz MJ, Vicente AM, Araico A, Dominguez JN, Terencio MC, Ferrándiz ML. Role of nuclear factor-κB and heme oxygenase-1 in the mechanism of action of an anti-inflammatory chalcone derivative in RAW 264.7 cells. Br J Pharmacol. 2004. 142:1191-1199.

Bauer M, Bauer I. Heme oxygenase-1: redox regulation and role in the hepatic response to oxidative stress. Antioxid Redox Signal. 2002. 4:749-758.

Bossy-Wetzel E, Schwarzenbacher R, Lipton SA. Molecular pathways to neurodegeneration. Nat Med. 2004. 10:S2-S9.

Cannistrà M, Ruggiero M, Zullo A, Gallelli G, Serafini S, Maria M, et al. Hepatic ischemia reperfusion injury: a systematic review of literature and the role of current drugs and biomarkers. Int J Surg. 2016. 33:S57-S70.

Chang CY, Cheng TJ, Chang FR, Wang HY, Kan WC, Li SL, et al. Macrophage mediated anti-proliferation effects of *Anthodia camphorata* non-polysaccharide based extracts on human hepatoma cells. Biosci Biotechnol Biochem. 2011. 75:624-632.

Chang YY, Liu YC, Kuo YH, Lin YL, Wu YS, Chen JW, et al. Effects of antrosterol from *Antrodia camphorata* submerged whole broth on lipid homeostasis, antioxidation, alcohol clearance, and anti-inflammation in livers of chronic-alcohol fed mice. J Ethnopharmacol. 2017. 202:200-207.

de Groot H, Rauen U. Ischemia-reperfusion injury: processes in pathogenetic networks: a review. Transplant Proc. 2007. 39: 481-484.

Donath MY, Shoelson SE. Type 2 diabetes as an inflammatory disease. Nat Rev Immunol. 2011. 11:98-107.

Esser N, Legrand-Poels S, Piette J, Scheen AJ, Paquot N. Inflammation as a link between obesity, metabolic syndrome and type 2 diabetes. Diabetes Res Clin Pract. 2014. 105:141-150.

Geethangili M, Tzeng YM. Review of pharmacological effects of *Antrodia camphorata* and its bioactive compounds. Evid Based Complement Alternat Med. 2011. 2011:212641. https://doi.org/10.1093/ecam/nep108

Hsieh YL, Wu SP, Fang LW, Hwang TS. Effects of *Antrodia camphorata* extracts on anti-oxidation, anti-mutagenesis and protection of DNA against hydroxyl radical damage. BMC Complement Altern Med. 2015. 15:237. https://doi.org/10.1186/s12906-015-0768-3

Huang GJ, Huang SS, Lin SS, Shao YY, Chen CC, Hou WC, et al. Analgesic effects and the mechanisms of anti-inflammation of ergostatrien-3β-ol from *Antrodia camphorata* submerged whole broth in mice. J Agric Food Chem. 2010. 58:7445-7452.

Jaeschke H, Smith CW. Mechanisms of neutrophil-induced parenchymal cell injury. J Leukoc Biol. 1997. 61:647-653.

Jaeschke H. Molecular mechanisms of hepatic ischemia-reperfusion injury and preconditioning. Am J Physiol Gastrointest Liver Physiol. 2003. 284:G15-G26.

Konishi T, Lentsch AB. Hepatic ischemia/reperfusion: mechanisms of tissue injury, repair, and regeneration. Gene Expr. 2017. 17:277-287.

Koo A, Komatsu H, Tao G, Inoue M, Guth PH, Kaplowitz N. Contribution of no-reflow phenomenon to hepatic injury after ischemia-reperfusion: evidence for a role for superoxide anion. Hepatology. 1992. 15:507-514.

Kuo YH, Lin CH, Shih CC. Ergostatrien-3β-ol from *Antrodia camphorata* inhibits diabetes and hyperlipidemia in high-fat-diet treated mice via regulation of hepatic related genes, glucose transporter 4, and AMP-activated protein kinase phosphorylation. J Agric Food Chem. 2015. 63:2479-2489.

Land WG. The role of postischemic reperfusion injury and other nonantigen-dependent inflammatory pathways in transplantation. Transplantation. 2005. 79:505-514.

Li S, Fujino M, Takahara T, Li XK. Protective role of heme oxygenase-1 in fatty liver ischemia-reperfusion injury. Med Mol Morphol. 2019. 52:61-72.

Liu B, Qian JM. Cytoprotective role of heme oxygenase-1 in liver ischemia reperfusion injury. Int J Clin Exp Med. 2015. 8: 19867-19873.

Liu YW, Lu KH, Ho CT, Sheen LY. Protective effects of *Antrodia cinnamomea* against liver injury. J Tradit Complement Med.

2012. 2:284-294.
National Research Council. Guide for the care and use of laboratory animals. 8th ed. National Academies Press, Washington, DC, USA. 2011. https://doi.org/10.17226/12910
Nickkholgh A, Li Z, Yi X, Mohr E, Liang R, Mikalauskas S, et al. Effects of a preconditioning oral nutritional supplement on pig livers after warm ischemia. HPB Surg. 2012. 2012:783479. https://doi.org/10.1155/2012/783479
Nitescu N, Ricksten SE, Marcussen N, Haraldsson B, Nilsson U, Basu S, et al. N-acetylcysteine attenuates kidney injury in rats subjected to renal ischaemia-reperfusion. Nephrol Dial Transplant. 2006. 21:1240-1247.
Pillai VG, Chen CL. Living donor liver transplantation in Taiwan-challenges beyond surgery. Hepatobiliary Surg Nutr. 2016. 5:145-150.
Rani V, Deep G, Singh RK, Palle K, Yadav UCS. Oxidative stress and metabolic disorders: pathogenesis and therapeutic strategies. Life Sci. 2016. 148:183-193.
Rao J, Qian X, Wang P, Pu L, Zhai Y, Wang X, et al. All-trans retinoic acid preconditioning protects against liver ischemia/reperfusion injury by inhibiting the nuclear factor kappa B signaling pathway. J Surg Res. 2013. 180:e99-e106.
Rubio-Perez JM, Morillas-Ruiz JM. A review: inflammatory process in Alzheimer's disease, role of cytokines. Sci World J. 2012. 2012:756357. https://doi.org/10.1100/2012/756357
Sepanlou SG, Safiri S, Bisignano C, Ikuta KS, Merat S, Saberifiroozi M, et al.; GBD 2017 Cirrhosis Collaborators. The global, regional, and national burden of cirrhosis by cause in 195 countries and territories, 1990-2017: a systematic analysis for the Global Burden of Disease Study 2017. Lancet Gastroenterol Hepatol. 2020. 5:245-266.
Shao YY, Chen CC, Wang HY, Chiu HL, Hseu TH, Kuo YH. Chemical constituents of *Antrodia camphorata* submerged whole broth. Nat Prod Res. 2008. 22:1151-1157.
Srisook K, Kim C, Cha YN. Molecular mechanisms involved in enhancing HO-1 expression: de-repression by heme and activation by Nrf2, the "one-two" punch. Antioxid Redox Signal. 2005. 7:1674-1687.
Taleb S. Inflammation in atherosclerosis. Arch Cardiovasc Dis. 2016. 109:708-715.
Tsai TC, Tung YT, Kuo YH, Liao JW, Tsai HC, Chong KY, et al. Anti-inflammatory effects of *Antrodia camphorata*, a herbal medicine, in a mouse skin ischemia model. J Ethnopharmacol. 2015. 159:113-121.
Walsh KB, Toledo AH, Rivera-Chavez FA, Lopez-Neblina F, Toledo-Pereyra LH. Inflammatory mediators of liver ischemia-reperfusion injury. Exp Clin Transplant. 2009. 7:78-93.
Weigand K, Brost S, Steinebrunner N, Büchler M, Schemmer P, Müller M. Ischemia/reperfusion injury in liver surgery and transplantation: pathophysiology. HPB Surg. 2012. 2012: 176723. https://doi.org/10.1155/2012/176723
Wu MT, Tzang BS, Chang YY, Chiu CH, Kang WY, Huang CH, et al. Effects of *Antrodia camphorata* on alcohol clearance and antifibrosis in livers of rats continuously fed alcohol. J Agric Food Chem. 2011. 59:4248-4254.
Yamauchi H, Baca I, Mittmann U, Geisen HP, Salzer M. Postischemic liver damage in rats: effect of some therapeutic interventions on survival rate. Tohoku J Exp Med. 1982. 138:63-70.
Yang HL, Korivi M, Chen CH, Peng WJ, Chen CS, Li ML, et al. *Antrodia camphorata* attenuates cigarette smoke-induced ROS production, DNA damage, apoptosis, and inflammation in vascular smooth muscle cells, and atherosclerosis in ApoE-deficient mice. Environ Toxicol. 2017. 32:2070-2084.
Yun N, Eum HA, Lee SM. Protective role of heme oxygenase-1 against liver damage caused by hepatic ischemia and reperfusion in rats. Antioxid Redox Signal. 2010. 13:1503-1512.